Available online at www.sciencedirect.com

ScienceDirect

Current Opinion in Electrochemistry

Review Article

Infrared nanoimaging and nanospectroscopy of electrochemical energy storage materials and interfaces

Jonathan M. Larson[1], Andrew Dopilka[2] and Robert Kostecki[2]

Abstract

Electrochemical interfaces are central to the function and performance of energy storage devices. Thus, the development of new methods to characterize these interfaces, in conjunction with electrochemical performance, is essential for bridging the existing knowledge gaps and accelerating the development of energy storage technologies. Of particular need is the ability to characterize surfaces or interfaces in a non-destructive way with adequate resolution to discern individual structural and chemical building blocks. To this end, sub-diffraction-limit low-energy infrared optical probes that exploit near-field interactions within atomic force microscopy platforms, such as pseudoheterodyne nanoimaging, photothermal nanoimaging and nanospectroscopy, and nanoscale Fourier transform infrared spectroscopy, are all powerful emerging techniques. These are capable of non-destructive surface probing and imaging at nanometer resolution. This review outlines recent efforts to characterize *ex situ,in situ,*and*operando* electrode materials and electrochemical interfaces in rechargeable batteries with these advanced infrared near-field probes.

Addresses

[1] Department of Chemistry and Biochemistry, Baylor University, Waco, TX, 76798, USA

[2] Energy Storage & Distributed Resources Division, Lawrence Berkeley National Laboratory, Berkeley, CA, 94720, USA

Corresponding authors: Kostecki, Robert (R_Kostecki@lbl.gov); Larson, Jonathan M. (Jonathan_Larson@Baylor.edu)

Current Opinion in Electrochemistry 2024, **47:**101548

This review comes from a themed issue on **Innovative Methods in Electrochemistry (2024)**

Edited by **Christine Kranz**

For complete overview about the section, refer Innovative Methods in Electrochemistry (2024)

Available online 3 June 2024

https://doi.org/10.1016/j.coelec.2024.101548

Keywords

Nano-FTIR, s-SNOM, SINS, AFM-IR, Infrared nanospectroscopy, Batteries, Li-ion battery, Energy storage, Electrochemistry.

Introduction

Critical to the advancement and realization of rechargeable high-energy density storage systems [1–5] is the fundamental understanding and control of the electrochemical interfaces which determine the function and operation of such devices [6–9]. Ideally, characterization of such dynamic interfaces [10], and the interphases that grow therein [11–13], would be done in an inherently non-destructive way, within its native environment, at spatial resolution that matches the size and distribution patterns, of the interphase individual building blocks. The practical realization of this goal is extremely challenging because these interfaces and interphases are: (i) buried at the junction of dissimilar materials — causing accessibility issues, (ii) highly reactive — causing stability issues, (iii) structurally and chemically heterogeneous — causing signal convolution issues, (iv) electrode potential dependent — causing controllability issues, and (v) nanometer-thin in contact with electrode and electrolyte — causing detectability and selectivity issues.

These analytical hurdles related to sensitivity, specificity, selectivity and environmental control stimulate the development of new experimental approaches to characterize electrochemical interfaces to overcome some subset of these challenges for a variety of specific materials and interface architectures. While a full survey of such endeavors is beyond the scope of this work, some notable examples employ X-ray [14–16], electron [17,18], neutron [19], optical [20–22], synchrotron [23], and scanning probe methods [24–26]. Provided herein, is a short review of an emerging class of infrared near-field nanoimaging and nanospectroscopy methodologies aimed at overcoming some of the aforementioned challenges to study electrochemical energy storage materials and interfaces, non-destructively, with nanoscale resolution, and in some cases, while within their native environment. Before moving to review specific experiments, we briefly discuss the working mechanisms and implementations of some of the common near-field approaches used on electrochemical systems.

Near-field probes based on atomic force microscope (AFM) platforms are capable of chemical imaging and

vibrational spectroscopy at resolutions below the diffraction-limit of the excitation wavelength [27,28]. Specific examples of these techniques include tip-enhanced Raman spectroscopy [29—31], and those that exploit infrared (IR) scattering (Figure 1a), or photothermal (PT) expansion (Figure 1b), from below a scanning probe's tip end. In the PT-type, typically pulsed IR light is directed at the tip/sample junction (Figure 1b), and induced local thermal expansion is detected and correlated with local IR absorption (Figure 1b, inset), and is referred to as AFM-IR [32—36]. Note that PTIR, PFIR, and PiFM are other photothermal modalities and have recently reviewed elsewhere [36]. The precise in-plane and out-of-plane spatial resolution for AFM-IR depends on the probe geometry and material, the sample material, and is still a point of research, but it is typically considered to be 10—20 nm and 100's of nm, respectively [35].

For the scattering-type, IR light is directed at the tip/sample junction (Figure 1a), the electric (near-) field is enhanced within nanoscopic regions around the probe tip's end (Figure 1a, inset), and backscattered light from that region is detected/processed with a combination of lock in demodulation and interferometric methods to obtain local optical properties such as reflection and absorption. The in-plane and out-of-plane spatial resolution for scattering-type depends on the probe geometry and material, the sample material, and (as with the PT-type) is still a point of research, but it is typically considered to be 10—20 nm and 10's of nm, respectively [38—40]. That said, the depth sensitivity is, in the least, highly dependent on (i) which demodulated harmonic is being considered (the higher harmonic, the shallower the probing depth [38—40]) and (ii) the dielectric properties of the sample material, where subsurface detection through insulators can be as deep as ca. 100 nm [41]. For metal samples, the fields decay rapidly so as to be mostly surface sensitive, however for nonmetal sample surfaces decorated with metal nanostructures, and/or nonmetal samples coated with low dimensional materials with resonant properties, subsurface detection depth can be tuned to some extent, amplifying surface and subsurface sensitivity [42—46].

Furthermore, properties of the incident light source (and detection methodology) permit various kinds of imaging and spectroscopy. If the IR light source is constant and monochromatic, scattering scanning near-field optical microscopy (s-SNOM) [47] capable of measuring local IR reflection and absorption at the energy of the incident light can be conducted. This approach is typically accomplished with a pseudoheterodyne detection scheme [48], and can be referred to in the literature as pseudoheterodyne imaging (PHI). If the incident light is energetically broadband, white light nanoimaging can be conducted which to first order maps gradients in local electronic conductivity, or nanoscale Fourier transform infrared spectroscopy (nano-FTIR) [49—51], or synchrotron infrared nanospectroscopy (SINS) [52,53] in cases where the incident broadband light originates from a synchrotron.

These relatively new and promising near-field probes for nanoscale vibrational imaging and spectroscopy are also generally non-destructive to the sample of interest as they typically operate in a tapping AFM mode, and the incident IR light has low photon energy. These approaches have been used to study a diversity of materials and physicochemical phenomena, including plasmons [54,55], phonon polaritons [56,57], dielectric properties [58], strain in low dimensional materials [59], COVID-19 virus [60], living cells [61], catalysts [62,63], and small molecule semiconductors [64]. This review focuses on research efforts that utilized near-field IR techniques to non-destructively characterize the structure and chemistry of electrochemical energy storage materials and interfaces with nanoscale resolution. In

Figure 1

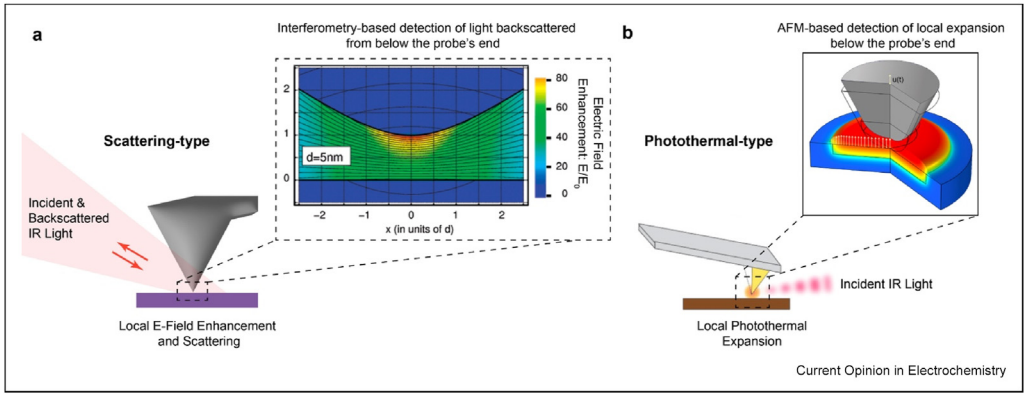

Schematic highlighting some of the key components of **(a)** s-SNOM-based and **(b)** photothermal-based IR nanoimaging and nanospectroscopy. Inset of (a) reproduced with permission [37] and display items in (b) reproduced with permission [35,36] (for inset).

the following four sections we review how IR near-field methods have been used to study (i) phase distributions within electrodes, (ii) electrolyte, coating, and membrane surfaces, (iii) *ex situ* interphases, and (iv) *in situ* and *operando* intact interfaces.

Phase distributions within electrodes

Electrodes (anodes and cathodes) are materials of central importance for energy storage as they reversibly store/dispense the electrochemically active species (typically Li) within a rechargeable battery. The first work to study an energy storage electrode with IR near-field measurements focused on illuminating phase distributions within lithium iron phosphate (LFP) microcrystals [65]. In the work the LFP microcrystals were characterized at various states of lithiation, with PHI-based nanospectroscopy [65]. The Li_xFePO_4 microcrystals were chemically delithiated to achieve a range of Li contents with values of x equal to 0, 0.5, 0.6, 0.74, and 1 (X-ray diffraction was used to determine x). Then, as shown in Figure 2a, near-field PHI-based nano-FTIR was conducted on fully lithiated and fully delithiated microcrystals, that is for x = 1 (LFP) and x = 0 (FP), respectively. This resulted in the identification of a very clear difference in their near-field spectra: a strong band from the near-field amplitude at about 1042 cm^{-1} in the fully lithiated case (note the amplitude is the absolute value of the complex-valued spectrum referenced to Si). This feature was then used in subsequent PHI and PHI-based nano-FTIR to (i) demonstrate a two-phase coexistence between local regions of more, or less, Li and (ii) elucidate the spatial distribution of these phases and mark the bounding interphase, all as a function of stochiometric amount of Li. As shown in Figure 2b, PHI at various states of lithiation exquisitely showcases the two-phase coexistence and geometric evolution of a diamond-shaped Li-rich phase. This was further confirmed with PHI-based nano-FTIR collected across the length of an ca. 2 micron long partially delithiated microcrystal with x = 0.74.

Electrolyte, coating, and membrane surfaces

IR nanoimaging has also been used for *ex situ* characterization of electrochemical surfaces. In this section we representatively cite some of these studies. Several works have utilized AFM-IR to characterize the

Figure 2

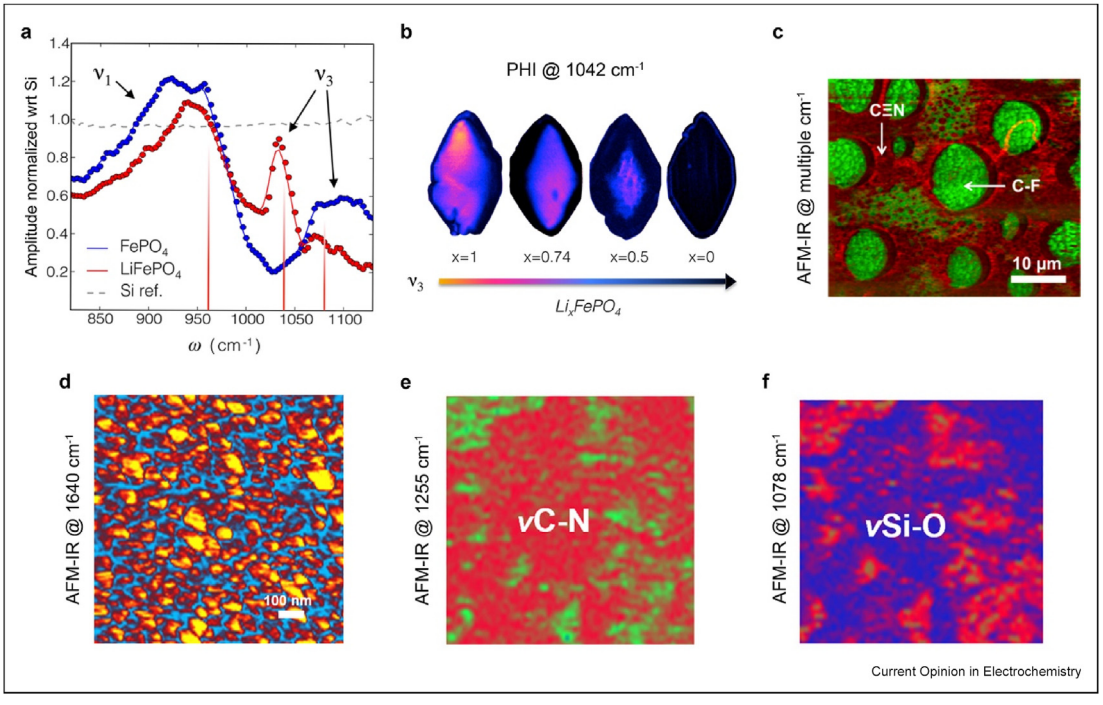

(a) PHI-based nano-FTIR of LFP and FP. Reproduced with permission [65]. **(b)** PHI at 1042 cm^{-1} of Li_xFePO_4 microcrystals at various states of lithiation. Reproduced with permission [65]. **(c)** The overlay of two AFM-IR images at ca. 1375 cm^{-1} and 2250 cm^{-1} for the identification of PVDF (-CF) and PAN (-CN), respectively, on the surface of a protective coating for Li anodes. Reproduced with permission [66]. **(d)** AFM-IR at 1640 cm^{-1} to map bicontinuous regions on the surface of polymer electrolyte membrane where blue (yellow) regions map P4VP/PA (PEEK) domains. Reproduced with permission [67]. **(e)** and **(f)**: AFM-IR at 1255 and 1078 cm^{-1}, respectively, for mapping C–N (from DMF) and Si–O vibrations (from MPS) on the surface of a PML electrolyte. Reproduced with permission [68]. (For interpretation of the references to color in this figure legend, the reader is referred to the Web version of this article.)

nanoscale distribution of chemical compounds in pristine polymer electrolytes, protective coatings, membranes, and composite electrolytes [66–71]. For example, the realization of metallic Li as an anode material requires developing new methods to stabilize the surface. A general proposed means toward this end is to use protective coating layers aimed at increasing stability. AFM-IR was recently used for chemical imaging of such a protective polymer coating used for stabilizing Li metal anodes [66]. The as-deposited coating, polyvinylidenefluoride polyacrylonitrile (PVDF–PAN), is lithiophilic, promotes uniform Li deposition, and possess porous structures arising from a phase segregation that can aid in Li-ion transport (Figure 2c) [66].

In another study, AFM-IR was used to characterize an as-prepared proton-conductive polymer electrolyte membrane possessing high stability and high conductivity required for high temperature supercapacitors [67]. The AFM-IR aided in the experimental confirmation of bicontinuous phases across the membrane surface (Figure 2d) that were prepared by controllable cross-linking of poly(ether-ether-ketone) and poly (4-vinylpyridine). An additional example of AFM-IR use in characterizing *ex situ* electrochemical surfaces is that of a recent study in which a polymer electrolyte surface chemistry was mapped [68]. The AFM-IR data clearly imaged and mapped heterogenous distributions of DMF and 3-methacryloxypropyltrimethoxysilane (MPS) along the surface of the pristine polymer electrolyte (Figure 2e,f) [68]. Other uses of AFM-IR include nanoimaging at 1712 cm^{-1} (corresponding to C=O stretching) to map the distribution of dimethylformamide in polyvinylidene electrolytes [72–76].

Ex situ interphases

A point of focus for near-field IR nanoimaging and nanospectroscopy efforts in the energy storage space has been the characterization of the solid-electrolyte interphase (SEI). The SEI formed on a Cu electrode after 1 cycle of Li metal plating and stripping in a 1 M LiFSI in 1,3-dioxolane (DOL) + 4 wt.% $LiNO_3$ electrolyte was characterized with AFM-IR nanoimaging [77]. Nanoimaging at 1081 cm^{-1} demonstrated a homogenous distribution of poly-DOL in the formed SEI layer. In another study, PHI was used to assess the spatial distribution of lithium ethylene dicarbonate (LiEDC) on the surface of a thin-film Si electrode after SEI formation in a 1.2 M $LiPF_6$ EC:EMC (at a 3:7 wt%) electrolyte [78]. By imaging at 1330, 1360, and 1410 cm^{-1}, the authors showed that the LiEDC randomly distributed on the surface suggests a high amount of SEI reaction heterogeneity.

Ex situ IR nanoimaging (with PHI) was conducted of the SEI on an Sn anode [79]. The Sn anode, in 1 M $LiPF_6$ in EC:DEC (at a 1:2 wt%) electrolyte, was cycled five times between 3V and 0.8V vs Li/Li^+ in an attempt to grow an SEI. The lower potential limit was chosen to prevent Sn–Li alloying. During cycling, large cathodic peaks around 1.3V vs Li/Li^+ suggested electrolyte reduction and SEI formation. However, their absolute current decreased with cycle number and cathodic peaks never vanished, implying imperfect surface passivation and reformation of SEI. Post cycling, the Sn electrode was removed from the beaker cell at ~3V, and transferred into the near-field system. Then, AFM of the SEI (Figure 3a), and PHI of the SEI was conducted at five energies: 1042, 1052, 1061, 1075, and 1088 cm^{-1}. The PHI at 1042 cm^{-1} is displayed in Figure 3b, showing IR evidence of nanoscale chemical heterogeneity of the SEI that is decoupled from the topography. PHI at the other energies showed the distribution of lithium carbonate (1088 cm^{-1}) and lithium ethylene dicarbonate (LEDC, 1061 cm^{-1}) within the SEI.

Ex situ PHI was carried out on the SEI on highly oriented pyrolytic graphite (HOPG) functioning as a model C anode [80]. Electrochemical protocols were the same as for the aforementioned Sn anode work[79]. However, in this case, the HOPG anode realized good passivation as demonstrated by cathodic reduction peaks becoming vanishingly small. AFM and PHI were collected of the SEI at three difference potentials vs Li/Li^+: 1.66, 1.36, and 0.9 V. These measurements revealed an SEI that comprised an inner and outer layer with distinct structural and optical properties (Figure 2c,d). The former was significantly smoother than the latter, yet still possessed a subtle chemical heterogeneity not correlated with its structure and only detectable with the near-field probe. At the higher potentials, the outer layer comprised an agglomerate of nanoparticles packed loosely enough for the inner SEI to be clearly observed (Figure 2c,d). While the nanoparticles ranged in size, their average diameter was close to 200 nm. Interestingly, with decreasing voltage, a densification and likely chemical evolution of the outer SEI film was observed at 0.9V, likely a key process in the stabilization of the SEI on carbon anodes.

Broadband nano-FTIR was utilized, in combination with AFM and white light nanoimaging, to study SEI layer formation on thin-film Si anodes, in a 1.2 M $LiPF_6$ EC:EMC (3:7 wt%) electrolyte [81]. The thin-films were investigated after cycling and a voltage hold to determine the SEI structure after formation and aging. The results of the characterization depended on whether the SEI was washed (with dimethyl carbonate) after cell disassembly. The washed SEI had a rougher topography, more heterogeneous white light reflectance, and altered nano-FTIR spectra (cf. Figure 3e,f) suggesting that washing the SEI, even briefly, can result in undesirable changes to the original SEI structure and topography. The non-washed SEI contained LiEDC, residual electrolyte, polyethylene oxide (PEO), and decomposition products derived from PF_6^- ions.

Figure 3

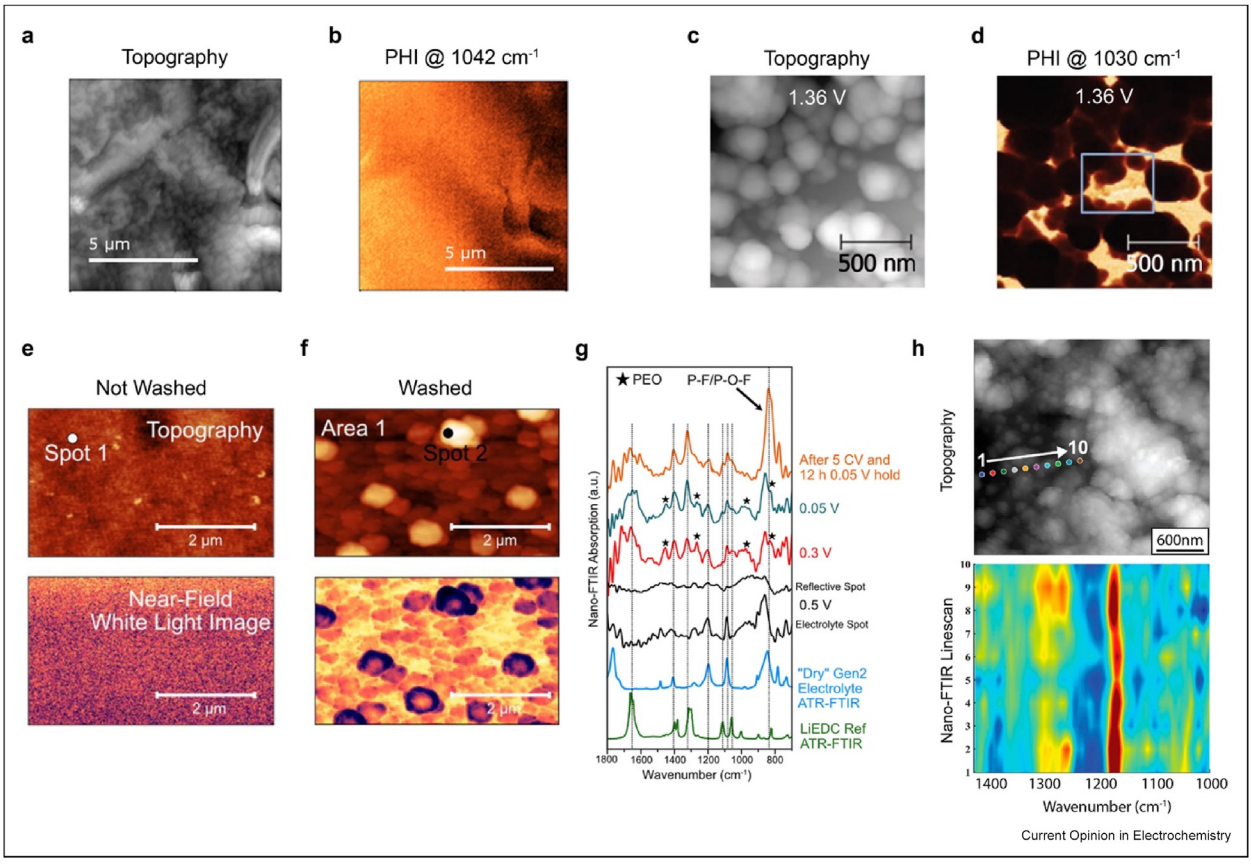

(a) Topography, via AFM, of the SEI on an Sn anode extracted at about 3V after 5 cycles and **(b)** PHI of the same at 1042 cm^{-1}, both reproduced with permission [79]. **(c)** AFM topography and **(d)** PHI at 1030 cm^{-1} of the SEI formed on an HOPG model carbon anode extracted at 1.36 V vs Li/Li^+, both reproduced with permission [80]. **(e)** and **(f)**: AFM topography (top), and near-field white light images (bottom) of the interphase on a thin-film Si electrode after cycling and aging with and without a washing treatment, respectively. Both reproduced with permission [81]. **(g)** Broadband nano-FTIR spectra of the interphase on a thin-film Si electrode taken at different potentials. Reproduced with permission [81]. **(h)** AFM (top) and nano-FTIR absorption (bottom) of a statically strained SEI on a delithiated to 1.5V vs Li/Li^+ thin-film Si anode. Both reproduced with permission [82].

Interestingly, the non-washed SEI was very chemically homogenous on the nanoscale suggesting that previously reported heterogeneity could arise from washing or other SEI altering treatments. Lastly, a comparison of the nano-FTIR spectra during the first lithiation and after electrochemical aging of the Si thin-film (Figure 3g) highlighted that PF_6^- ions and its decomposition products were accumulating within the SEI layer, implicating the anion as a major contributor to parasitic reactions during aging.

In order to conduct nano-FTIR across SEIs on model Si anodes that possessed different amounts of static strain, and at various potentials with respect to Li/Li^+, a new methodology amenable to near-field characterization was devised and implemented [82]. This was accomplished by fabricating custom model thin-film Si anodes atop Li-ion inert materials that were either mechanically compliant/soft (polydimethylsiloxane) or mechanically rigid/hard (fused silica). When undergoing electrochemical lithiation, the thin-film Si anode on the soft substrate, and the SEI residing thereon, wrinkled and experienced a peak biaxial strain of ca. 10%., whilst the Si anode on the hard substrate did not experience in−plain strain. Electrochemical measurements comparing the parasitic currents realized in each system, at multiple potentials vs Li/Li^+ below 0.8V, showed that the statically strained SEI experienced 10−25% more parasitic current. Subsequent AFM (Figure 3h, top) and nano-FTIR (Figure 3h, bottom) measurements of the strained SEIs suggest that the strained SEI experiences a structural loosing that opens nanochannels and facilitates the selective penetration and confinement of EMC to the surface of the Si electrode. As a result of, and after these processes, solvent reduction and electrolyte decomposition continues at the Si electrode, increasing parasitic electrolyte reduction current on Si and negatively influencing calendar life for Si anode batteries.

In situ and *operando* intact interfaces

So far, in the previous section, we discussed *ex situ* methods for characterizing interphases. In this section, we review reports of *in situ* and *operando* characterization of electrochemical interfaces, and also, in some cases, the interphases that grow therein. A recent work [83] describes the fabrication of ultrathin free-standing IR and electron transparent metal-oxide membranes for use in studies of solid−gas and solid−liquid interfaces (Figure 4a, inset). Notably, they fabricate a free-standing graphene/TiO_2 membrane by transferring graphene onto a porous array of 1-um diameter holes and then depositing 2 nm of TiO_2 onto the graphene with plasma-enhanced atomic layer deposition. Using ultrabroadband SINS, they probed the graphene/TiO_2/sodium sulfate (0.1 M in H_2O) interface which revealed absorption from the antisymmetric stretching mode of S═O around 1100 cm^{-1} and the H−O−H bending mode at 1650 cm^{-1} with altered peak intensities relative to the bulk ATR-FTIR spectrum. The difference from the bulk is attributed to the modified structure of the electric double layer at the TiO_2/sodium sulfate interface being probed by the local near-field (Figure 1a). This work

Figure 4

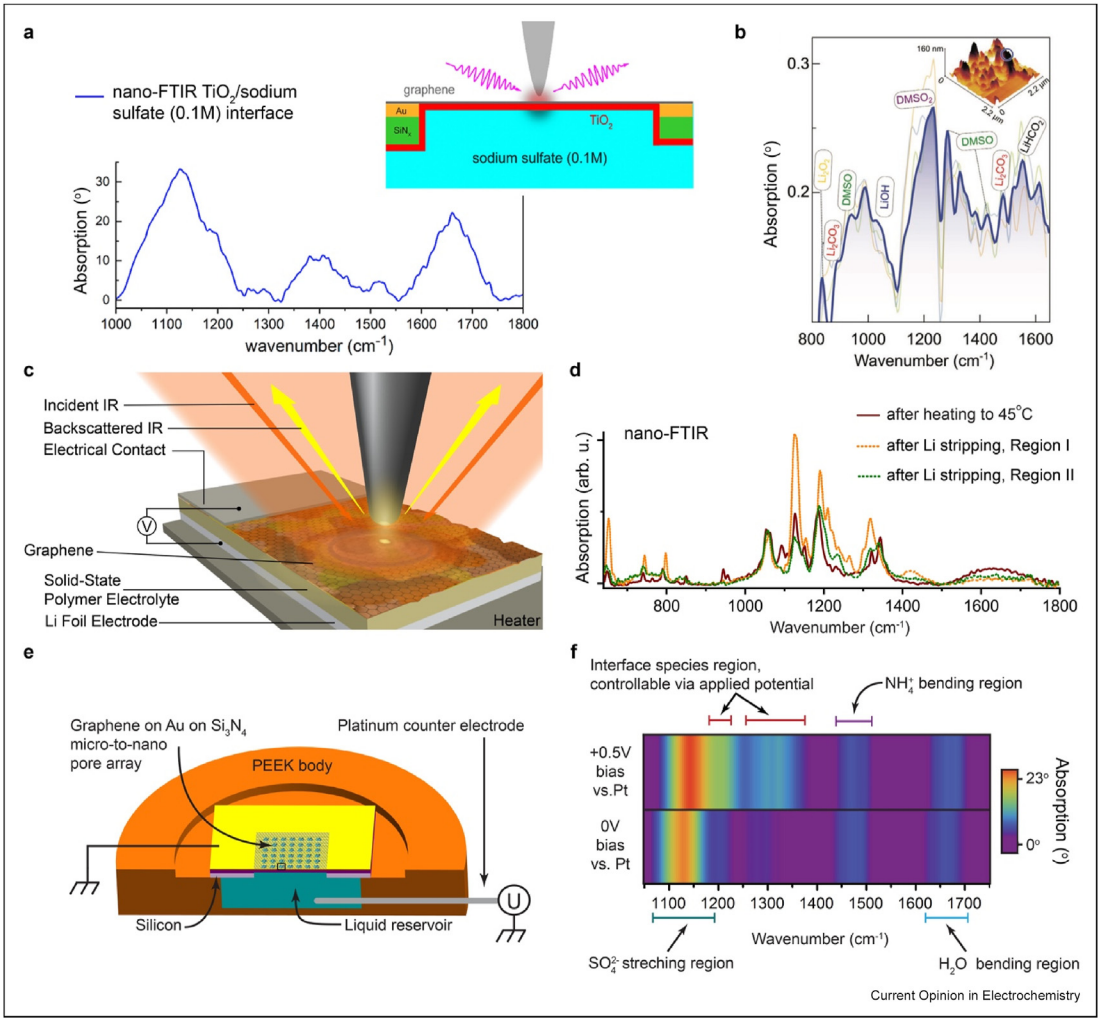

(a) Nano-FTIR absorption spectrum (and schematic, inset) of titanium oxide/electrolyte interface. Reproduced with permission [83]. **(b)** SINS absorption spectrum of a three-phase interface in a Li-air battery. Reproduced with permission [84]. **(c)** Three-dimensional rendering of a graphene-enabling anode-free device for characterizing Li-polymer electrolyte interphases *in situ* with nano-FTIR. Reproduced with permission [85]. **(d)** Nano-FTIR spectra of the pristine polymer electrolyte and two regions of the Li-polymer electrolyte interphase. Reproduced with permission [85]. **(e)** Three-dimensional rendering of a graphene-enabling device for *in situ* or *operando* IR imaging or nanospectroscopy with simultaneous bulk electrochemical control. Reproduced with permission [86]. **(f)** Nano-FTIR absorption spectra of an electrochemically active solid–liquid electrolyte interface, *operando,* during bulk potential step experiments between 0 and 0.5 V. Simultaneous control and spectroscopic characterization of the relative concentration of species in the electric double layer is demonstrated. Reproduced with permission [86].

provides an important experimental blueprint for characterizing model metal-oxide/electrolyte interfaces.

In situ SINS was used to characterize the complex three-phase zone of a Li-air battery (Figure 4b) [84]. This three-phase zone refers to the interface between carbon nanotubes, electrolyte, and gas. SINS measurements were conducted at the three-phase zone after galvanostatic discharge at 1.28 μ Ah cm^{-2} and immediate transfer into the SINS sample stage under inert conditions. The multiscale analysis done in this work (via SINS and micro-FTIR) demonstrated that even with the heterogeneity present on the cathode surface, the discharge rate did not influence discharge products. Moreover, evidence of electrolyte degradation and formate species formation was also found.

Another work that leveraged nano-FTIR [85] started by fabricating a custom anode-free battery device (Figure 4c) which, in the as-prepared state, was made up of a stainless steel current collector, monolayer graphene, a polymer electrolyte, and Li metal on a stainless current collector, all on a heating plate. The graphene functioned as both an electrode and IR transparent window. Li functioned as both counter and reference. Li was galvanostatically plated onto the graphene, generating an Li/polymer electrolyte interface which then reacted to form an interphase. Nano-FTIR characterization was done in the pristine, post-heating, post-plating, and post-stripping states, *in situ*, and revealed that (i) nanoscale heterogeneities along the polymer electrolyte surface led to heterogenous Li plating and SEI formation, (ii) the PEO in the interphase region becomes fully amorphous, and (iii) the SEI is primarily composed of chemically distinct regions (Figure 4d).

In order to enable multimodal characterizations of liquids and solid/liquid interfaces in their native environment, a custom liquid cell device (Figure 4e) amenable for IR nanoimaging and nanospectroscopy of liquids and electrochemically controlled graphene/liquid interfaces was constructed [86]. *In situ* SINS measurements were conducted on water and propylene carbonate. *Operando* SINS measurements were conducted at the graphene/ammonium sulfate in water-electrolyte interface. Specifically, during tens of potential step experiments between 0.5V and 0V. The *operando* data revealed that interface species likely from the electric double layer around 1200 and 1300 cm^{-1} were reversibly electrochemically manipulable and detectible with infrared nanospectroscopy (Figure 4f).

Concluding remarks

As demonstrated by the above-described works, near-field IR nanoimaging and nanospectroscopy clearly hold promise for future characterization of energy storage materials and interfaces. That said, there are certainly challenges associated with implementing these techniques that should be mentioned. For example, the z-piezo max scan range is usually somewhere between 1 and 10 micron, and so the sample areas of interest need to be flat enough to be compatible with such ranges. The sample thickness is also something that needs to be carefully considered as the total allowed thickness is often between 5 and 20 mm. This constraint becomes increasingly challenging when trying to design custom compatible devices. Combine these with the fact that the approach is necessarily a combination of AFM and IR imaging and spectroscopy, and it becomes clear that the approach is not a plug-and-play technique. On the other hand, players in the commercialization of the technology are making notable strides in lowering the barrier to entry and offering robust solutions; and the technical merits and unique capability of the analytical technique shouldn't be overlooked. Furthermore, the realization of *in situ* and *operando* electrochemistry plus near-field IR nanoimaging and nanospectroscopy is in its infancy, and holds great promise for unearthing insights in the basic science of energy storage interfaces and interphases.

Indeed, moving toward the characterization of electrochemically controlled surfaces and interfaces in rechargeable battery materials and systems is critical for catalyzing advanced energy storage technologies. Holding promise on this front is implementing methods that are inherently non-destructive, capable of nanoscale resolution over microscale regions, and amenable to characterization of surfaces and interfaces while in their native environment. Herein we outlined recent efforts progressing to this end based on infrared near-field probes. We briefly discussed the working mechanisms and implementations of the scattering- and photothermal-types, and highlighted works in which these tools were employed to characterize (i) phase distributions within electrodes, (ii) electrolyte, coating, and membrane surfaces, (iii) *ex situ* interphases, and (iv) *in situ* and *operando* intact interfaces. The latter approaches were enabled by the integration of bulk electrochemistry and custom nanofabrication, with near-field IR nanoimaging and/or spectroscopy. These near-field IR multimodal characterization schemes will no doubt be applied to more energy storage systems and chemistries in the future, and their capabilities expanded further still, so even more critically important physicochemical properties hidden at energy storage surfaces and interfaces will come to light.

Declaration of competing interest

The authors declare that they have no known competing financial interests or personal relationships that could have appeared to influence the work reported in this paper.

Data availability

No data were used for the research described in the article.

Acknowledgements

This work was supported by the Assistant Secretary for Energy Efficiency and Renewable Energy, Office of Vehicle Technologies of the US Department of Energy under Contract No. DE-AC02-05CH11231, under the Battery Materials Research program, directed by Tien Duong (RK), and the Silicon Consortium Program, directed by B. Cunningham (RK and AD). J.M.L. acknowledges Baylor University for financial support through startup funds.

References

Papers of particular interest, published within the period of review, have been highlighted as:

* of special interest
** of outstanding interest

1. Zhao Z, Alshareef HN: **Sustainable dual-ion batteries beyond Li**. *Adv Mater* 2024, **36**, e2309223.
2. Gao Y, Pan Z, Sun J, Liu Z, Wang J: **High-energy batteries: beyond lithium-ion and their long road to commercialisation**. *Nano-Micro Lett* 2022, **14**:94.
3. Aziam H, Larhrib B, Hakim C, Sabi N, Ben Youcef H, Saadoune I: **Solid-state electrolytes for beyond lithium-ion batteries: a review**. *Renew Sustain Energy Rev* 2022, **167**, 112694.
4. Tian Y, Zeng G, Rutt A, Shi T, Kim H, Wang J, Koettgen J, Sun Y, Ouyang B, Chen T, *et al.*: **Promises and challenges of next-generation "beyond Li-ion" batteries for electric vehicles and grid decarbonization**. *Chem Rev* 2021, **121**:1623–1669.
5. Cabana J, Monconduit L, Larcher D, Palacin MR: **Beyond intercalation-based Li-ion batteries: the state of the art and challenges of electrode materials reacting through conversion reactions**. *Adv Mater* 2010, **22**:E170–E192.
6. Chen C, Jiang M, Zhou T, Raijmakers L, Vezhlev E, Wu B, Schülli TU, Danilov DL, Wei Y, Eichel RA, Notten PHL: **Interface aspects in all-solid-state Li-based batteries reviewed**. *Adv Energy Mater* 2021, **11**, 2003939.
7. Yan C, Yuan H, Park HS, Huang J-Q: **Perspective on the critical role of interface for advanced batteries**. *J Energy Chem* 2020, **47**:217–220.
8. Yan C, Xu R, Xiao Y, Ding JF, Xu L, Li BQ, Huang JQ: **Toward critical electrode/electrolyte interfaces in rechargeable batteries**. *Adv Funct Mater* 2020, **30**, 1909887.
9. Xiao Y, Wang Y, Bo S-H, Kim JC, Miara LJ, Ceder G: **Understanding interface stability in solid-state batteries**. *Nat Rev Mater* 2020, **5**:105–126.
10. Li Y, Gao Z, Hu F, Lin X, Wei Y, Peng J, Yang J, Li Z, Huang Y, Ding H: **Advanced characterization techniques for interface in all-solid-state batteries**. *Small Methods* 2020, **4**, 2000111.
11. Kühn SP, Pfeiffer F, Bela M, Rodehorst U, Weintz D, Stan M, Baghernejad M, Winter M, Cekic-Laskovic I: **Back to the basics: advanced understanding of the as-defined solid electrolyte interphase on lithium metal electrodes**. *J Power Sources* 2022, **549**, 232118.
12. Xu K: **Electrolytes and interphases in Li-ion batteries and beyond**. *Chem Rev* 2014, **114**:11503–11618.
13. Winter M: **The solid electrolyte interphase – the most important and the least understood solid electrolyte in rechargeable Li batteries**. *Z Phys Chem* 2009, **223**:1395–1406.
14. Simon FJ, Hanauer M, Richter FH, Janek J: **Interphase Formation of PEO20:LiTFSI-Li6PS5Cl composite electrolytes with lithium metal**. *ACS Appl Mater Interfaces* 2020, **12**:11713–11723.
15. Dietrich C, Koerver R, Gaultois MW, Kieslich G, Cibin G, Janek J, Zeier WG: **Spectroscopic characterization of lithium thiophosphates by XPS and XAS - a model to help monitor interfacial reactions in all-solid-state batteries**. *Phys Chem Chem Phys* 2018, **20**:20088–20095.
16. Seitzman N, Guthrey H, Sulas DB, Platt HAS, Al-Jassim M, Pylypenko S: **Toward all-solid-state lithium batteries: three-dimensional visualization of lithium migration in β-Li3PS4 ceramic electrolyte**. *J Electrochem Soc* 2018, **165**: A3732–A3737.
17. Cheng DY, Wynn TA, Wang XF, Wang S, Zhang MH, Shimizu R, Bai S, Nguyen H, Fang CC, Kim MC, *et al.*: **Unveiling the stable nature of the solid electrolyte interphase between lithium metal and LiPON via cryogenic electron microscopy**. *Joule* 2020, **4**:2484–2500.
18. Ma C, Cheng Y, Yin K, Luo J, Sharafi A, Sakamoto J, Li J, More KL, Dudney NJ, Chi M: **Interfacial stability of Li metal-solid electrolyte elucidated via in situ electron microscopy**. *Nano Lett* 2016, **16**:7030–7036.
19. Wang C, Gong Y, Dai J, Zhang L, Xie H, Pastel G, Liu B, Wachsman E, Wang H, Hu L: **In situ neutron depth profiling of lithium metal-garnet interfaces for solid state batteries**. *J Am Chem Soc* 2017, **139**:14257–14264.
20. Amaral MM, Real CG, Yukuhiro VY, Doubek G, Fernandez PS, Singh G, Zanin H: **In situ and operando infrared spectroscopy of battery systems: progress and opportunities**. *J Energy Chem* 2023, **81**:472–491.
21. Cowan AJ, Hardwick LJ: **Advanced spectroelectrochemical techniques to study electrode interfaces within lithium-ion and lithium-oxygen batteries**. *Annu Rev Anal Chem* 2019, **12**: 323–346.
22. Sang LZ, Haasch RT, Gewirth AA, Nuzzo RG: **Evolution at the solid electrolyte/gold electrode interface during lithium deposition and stripping**. *Chem Mater* 2017, **29**:3029–3037.
23. Black AP, Sorrentino A, Fauth F, Yousef I, Simonelli L, Frontera C, Ponrouch A, Tonti D, Palacin MR: **Synchrotron radiation based operando characterization of battery materials**. *Chem Sci* 2023, **14**:1641–1665.
24. Chen X, Lai J, Shen Y, Chen Q, Chen L: **Functional scanning force microscopy for energy nanodevices**. *Adv Mater* 2018, **30**, e1802490.
25. Takahashi Y, Kumatani A, Shiku H, Matsue T: **Scanning probe microscopy for nanoscale electrochemical imaging**. *Anal Chem* 2017, **89**:342–357.
26. Danis L, Gateman SM, Kuss C, Schougaard SB, Mauzeroll J: **Nanoscale measurements of lithium-ion-battery materials using scanning probe techniques**. *Chemelectrochem* 2017, **4**: 6–19.
27. Xiao L, Schultz ZD: **Spectroscopic imaging at the nanoscale: Technologies and recent applications**. *Anal Chem* 2018, **90**: 440–458.
28. Muller EA, Pollard B, Raschke MB: **Infrared chemical nano-imaging: accessing structure, coupling, and dynamics on molecular length scales**. *J Phys Chem Lett* 2015, **6**:1275–1284.
29. Touzalin T, Joiret S, Maisonhaute E, Lucas IT: **Capturing electrochemical transformations by tip-enhanced Raman spectroscopy**. *Curr Opin Electrochem* 2017, **6**:46–52.
30. Wang YZ, Wang J, Wang X, Ren B: **Electrochemical tip-enhanced Raman spectroscopy for in situ study of electrochemical systems at nanoscale**. *Curr Opin Electrochem* 2023, **42**, 101385.
31. Kurouski D, Dazzi A, Zenobi R, Centrone A: **Infrared and Raman chemical imaging and spectroscopy at the nanoscale**. *Chem Soc Rev* 2020, **49**:3315–3347.
32. Schwartz JJ, Jakob DS, Centrone A: **A guide to nanoscale IR spectroscopy: resonance enhanced transduction in contact and tapping mode AFM-IR**. *Chem Soc Rev* 2022, **51**: 5248–5267.
33. Donaldson PM, Kelley CS, Frogley MD, Filik J, Wehbe K, Cinque G: **Broadband near-field infrared spectromicroscopy using photothermal probes and synchrotron radiation**. *Opt Express* 2016, **24**:1852–1864.

34. Dazzi A, Prater CB: **AFM-IR: technology and applications in nanoscale infrared spectroscopy and chemical imaging**. *Chem Rev* 2017, **117**:5146–5173.

35. Mathurin J, Deniset-Besseau A, Bazin D, Dartois E, Wagner M, Dazzi A: **Photothermal AFM-IR spectroscopy and imaging: status, challenges, and trends**. *J Appl Phys* 2022, **131**, 010901.

36. Xie Q, Xu XG: **What do different modes of AFM-IR mean for measuring soft matter surfaces?** *Langmuir* 2023, **39**: 17593–17599.

37. Behr N, Raschke MB: **Optical antenna properties of scanning probe tips: plasmonic light scattering, Tip–Sample coupling, and near-field enhancement**. *J Phys Chem C* 2008, **112**: 3766–3773.

38. Govyadinov AA, Mastel S, Golmar F, Chuvilin A, Carney PS, Hillenbrand R: **Recovery of permittivity and depth from near-field data as a step toward infrared nanotomography**. *ACS Nano* 2014, **8**:6911–6921.

39. Mooshammer F, Huber MA, Sandner F, Plankl M, Zizlsperger M, Huber R: **Quantifying nanoscale electromagnetic fields in near-field microscopy by fourier demodulation analysis**. *ACS Photonics* 2020, **7**:344–351.

40. Krutokhvostov R, Govyadinov AA, Stiegler JM, Huth F, Chuvilin A, Carney PS, Hillenbrand R: **Enhanced resolution in subsurface near-field optical microscopy**. *Opt Express* 2012, **20**:593–600.

41. Mester L, Govyadinov AA, Chen S, Goikoetxea M, Hillenbrand R: **Subsurface chemical nanoidentification by nano-FTIR spectroscopy**. *Nat Commun* 2020, **11**:3359.

42. Li P, Wang T, Bockmann H, Taubner T: **Graphene-enhanced infrared near-field microscopy**. *Nano Lett* 2014, **14**:4400–4405.

43. Li P, Lewin M, Kretinin AV, Caldwell JD, Novoselov KS, Taniguchi T, Watanabe K, Gaussmann F, Taubner T: **Hyperbolic phonon-polaritons in boron nitride for near-field optical imaging and focusing**. *Nat Commun* 2015, **6**:7507.

44. Hu Y, López-Lorente ÁI, Mizaikoff B: **Graphene-based surface enhanced vibrational spectroscopy: recent developments, challenges, and applications**. *ACS Photonics* 2019, **6**: 2182–2197.

45. Yao Z, Chen X, Wehmeier L, Xu S, Shao Y, Zeng Z, Liu F, McLeod AS, Gilbert Corder SN, Tsuneto M, *et al.*: **Probing subwavelength in-plane anisotropy with antenna-assisted infrared nano-spectroscopy**. *Nat Commun* 2021, **12**:2649.

46. Wilcken R, Nishida J, Triana JF, John-Herpin A, Altug H, Sharma S, Herrera F, Raschke MB: **Antenna-coupled infrared nanospectroscopy of intramolecular vibrational interaction**. *Proc Natl Acad Sci U S A* 2023, **120**, e2220852120.

47. Chen X, Hu D, Mescall R, You G, Basov DN, Dai Q, Liu M: **Modern scattering-type scanning near-field optical microscopy for advanced material research**. *Adv Mater* 2019, **31**, 1804774.

48. Ocelic N, Huber A, Hillenbrand R: **Pseudoheterodyne detection for background-free near-field spectroscopy**. *Appl Phys Lett* 2006, **89**, 101124.

49. Huth F, Govyadinov A, Amarie S, Nuansing W, Keilmann F, Hillenbrand R: **Nano-FTIR absorption spectroscopy of molecular fingerprints at 20 nm spatial resolution**. *Nano Lett* 2012, **12**:3973–3978.

50. Amarie S, Zaslansky P, Kajihara Y, Griesshaber E, Schmahl WW, Keilmann F: **Nano-FTIR chemical mapping of minerals in biological materials**. *Beilstein J Nanotechnol* 2012, **3**:312–323.

51. Stiegler JM, Abate Y, Cvitkovic A, Romanyuk YE, Huber AJ, Leone SR, Hillenbrand R: **Nanoscale infrared absorption spectroscopy of individual nanoparticles enabled by scattering-type near-field microscopy**. *ACS Nano* 2011, **5**:6494–6499.

52. Bechtel HA, Muller EA, Olmon RL, Martin MC, Raschke MB: **Ultrabroadband infrared nanospectroscopic imaging**. *Proc Natl Acad Sci U S A* 2014, **111**:7191–7196.

53. Bechtel HA, Johnson SC, Khatib O, Muller EA, Raschke MB: **Synchrotron infrared nano-spectroscopy and -imaging**. *Surf Sci Rep* 2020, **75**, 100493.

54. Fei Z, Rodin AS, Andreev GO, Bao W, McLeod AS, Wagner M, Zhang LM, Zhao Z, Thiemens M, Dominguez G, *et al.*: **Gate-tuning of graphene plasmons revealed by infrared nano-imaging**. *Nature* 2012, **487**:82–85.

55. Ni GX, McLeod AS, Sun Z, Wang L, Xiong L, Post KW, Sunku SS, Jiang BY, Hone J, Dean CR, *et al.*: **Fundamental limits to graphene plasmonics**. *Nature* 2018, **557**:530–533.

56. Fali A, White ST, Folland TG, He M, Aghamiri NA, Liu S, Edgar JH, Caldwell JD, Haglund RF, Abate Y: **Refractive index-based control of hyperbolic phonon-polariton propagation**. *Nano Lett* 2019, **19**:7725–7734.

57. Dai S, Fei Z, Ma Q, Rodin AS, Wagner M, McLeod AS, Liu MK, Gannett W, Regan W, Watanabe K, *et al.*: **Tunable phonon polaritons in atomically thin van der Waals crystals of boron nitride**. *Science* 2014, **343**:1125–1129.

58. Fali A, Gamage S, Howard M, Folland TG, Mahadik NA, Tiwald T, Bolotin K, Caldwell JD, Abate Y: **Nanoscale spectroscopy of dielectric properties of mica**. *ACS Photonics* 2020, **8**:175–181.

59. Lyu B, Li H, Jiang L, Shan W, Hu C, Deng A, Ying Z, Wang L, Zhang Y, Bechtel HA, *et al.*: **Phonon polariton-assisted infrared nanoimaging of local strain in hexagonal boron nitride**. *Nano Lett* 2019, **19**:1982–1989.

60. O'Callahan B, Qafoku O, Balema V, Negrete OA, Passian A, Engelhard MH, Waters KM: **Atomic force microscopy and infrared nanospectroscopy of COVID-19 spike protein for the quantification of adhesion to common surfaces**. *Langmuir* 2021, **37**:12089–12097.

61. Kaltenecker KJ, Golz T, Bau E, Keilmann F: **Infrared-spectroscopic, dynamic near-field microscopy of living cells and nanoparticles in water**. *Sci Rep* 2021, **11**, 21860.

62. Ni GX, Chen S, Sunku SS, Sternbach A, McLeod AS, Xiong L, Fogler MM, Chen G, Basov DN: **Nanoscale infrared spectroscopy and imaging of catalytic reactions in Cu2O crystals**. *ACS Photonics* 2020, **7**:576–580.

63. Wu CY, Wolf WJ, Levartovsky Y, Bechtel HA, Martin MC, Toste FD, Gross E: **High-spatial-resolution mapping of catalytic reactions on single particles**. *Nature* 2017, **541**:511–515.

64. Rao VJ, Matthiesen M, Goetz KP, Huck C, Yim C, Siris R, Han J, Hahn S, Bunz UHF, Dreuw A, *et al.*: **AFM-IR and IR-SNOM for the characterization of small molecule organic semiconductors**. *J Phys Chem C* 2020, **124**:5331–5344.

65. ** Lucas IT, McLeod AS, Syzdek JS, Middlemiss DS, Grey CP, Basov DN, Kostecki R: **IR near-field spectroscopy and imaging of single Li(x)FePO4 microcrystals**. *Nano Lett* 2015, **15**:1–7.
First IR near-field measurements of an energy storage electrode. IR near-field tomography of two phase Li(x)FePO4 microcrystals.

66. Wang D, Liu H, Liu F, Ma G, Yang J, Gu X, Zhou M, Chen Z: **Phase-separation-induced porous lithiophilic polymer coating for high-efficiency lithium metal batteries**. *Nano Lett* 2021, **21**:4757–4764.

67. Zeng M, Guo H, Wang G, Shang L, Zhao C, Li H: **Nanostructured high-performance electrolyte membranes based on polymer network post-assembly for high-temperature supercapacitors**. *J Colloid Interface Sci* 2021, **603**:408–417.

68. Zhao L, Yu XN, Jiao JY, Song X, Cheng X, Liu M, Wang LL, Zheng JX, Lv W, Zhong GM, *et al.*: **Building cross-phase ion transport channels between ceramic and polymer for highly conductive composite solid-state electrolyte**. *Cell Reports Physical Science* 2023, **4**, 101382.

69. Xue C, Zhang X, Wang S, Li L, Nan CW: **Organic-organic composite electrolyte enables ultralong cycle life in solid-state lithium metal batteries**. *ACS Appl Mater Interfaces* 2020, **12**:24837–24844.

70. Fan YZ, Li RH, Yi RW, Zheng L, Wang JS, Huang R, Gong ZM, Li ZY, Qi JZ, Liu X, *et al.*: **Surface-dipole-directed formation of stable solid electrolyte interphase**. *Cell Reports Physical Science* 2023, **4**, 101324.

71. Liu Y, An X, Yang K, Ma J, Mi J, Zhang D, Cheng X, Li Y, Ma Y, Liu M, *et al.*: **Achieving a high loading of cathode in PVDF-based solid-state battery**. *Energy Environ Sci* 2024, **17**:344–353.

72. Zhang X, Han J, Niu X, Xin C, Xue C, Wang S, Shen Y, Zhang L, Li L, Nan CW: **High cycling stability for solid-state Li metal batteries via regulating solvation effect in poly(vinylidene fluoride)-based electrolytes**. *Batteries & Supercaps* 2020, **3**: 876–883.

73. Yang K, Chen L, Ma J, Lai C, Huang Y, Mi J, Biao J, Zhang D, Shi P, Xia H, *et al.*: **Stable interface chemistry and multiple ion transport of composite electrolyte contribute to ultra-long cycling solid-state LiNi(0.8) Co(0.1) Mn(0.1) O(2)/lithium metal batteries**. *Angew Chem Int Ed Engl* 2021, **60**:24668–24675.

74. Xue CJ, Guan SD, Hu BK, Wang XZ, Xin CZ, Liu SJ, Yu JY, Wen KH, Li LL, Nan CW: **Significantly improved interface between PVDF-based polymer electrolyte and lithium metal via thermal-electrochemical treatment**. *Energy Storage Mater* 2022, **46**:452–460.

75. An X, Liu Y, Yang K, Mi J, Ma J, Zhang D, Chen L, Liu X, Guo S, Li Y, *et al.*: **Dielectric filler-induced hybrid interphase enabling robust solid-state Li metal batteries at high areal capacity**. *Adv Mater* 2024, **36**, e2311195.

76. Wu Q, Fang M, Jiao S, Li S, Zhang S, Shen Z, Mao S, Mao J, Zhang J, Tan Y, *et al.*: **Phase regulation enabling dense polymer-based composite electrolytes for solid-state lithium metal batteries**. *Nat Commun* 2023, **14**:6296.

77. Jie YL, Xu YL, Chen YW, Xie M, Liu Y, Huang FY, Kochovski Z, Lei ZW, Zheng L, Song PD, *et al.*: **Molecular understanding of interphase formation via operando polymerization on lithium metal anode**. *Cell Reports Physical Science* 2022, **3**, 101057.

78. Hasa I, Haregewoin AM, Zhang L, Tsai WY, Guo J, Veith GM, Ross PN, Kostecki R: **Electrochemical reactivity and passivation of Silicon thin-film electrodes in organic carbonate electrolytes**. *ACS Appl Mater Interfaces* 2020, **12**:40879–40890.

79. ** Ayache M, Lux SF, Kostecki R: **IR near-field study of the solid electrolyte interphase on a tin electrode**. *J Phys Chem Lett* 2015, **6**:1126–1129.
First IR near-field measurements of an SEI layer.

80. * Ayache M, Jong D, Syzdek J, Kostecki R: **Near-field IR nanoscale imaging of the solid electrolyte interphase on a Hopg electrode**. *J Electrochem Soc* 2015, **162**:A7078–A7082.
First IR near-field measurements of the SEI on a model carbon anode.

81. ** Dopilka A, Gu Y, Larson JM, Zorba V, Kostecki R: **Nano-FTIR spectroscopy of the solid electrolyte interphase layer on a thin-film Silicon Li-ion anode**. *ACS Appl Mater Interfaces* 2023, **15**:6755–6767.
First IR nanospectroscopy of an *ex situ* SEI layer demonstrating the important effects of electrode washing and its relationship to nanoscale heterogenity.

82. * Yoon I, Larson JM, Kostecki R: **The effect of the SEI layer mechanical deformation on the passivity of a Si anode in organic carbonate electrolytes**. *ACS Nano* 2023, **17**: 6943–6954.
Discovered how static strain in SEIs on Si anodes influence's parasitic current and calendar life.

83. * Lu YH, Morales C, Zhao X, van Spronsen MA, Baskin A, Prendergast D, Yang P, Bechtel HA, Barnard ES, Ogletree DF, *et al.*: **Ultrathin free-standing oxide membranes for electron and photon spectroscopy studies of solid-gas and solid-liquid interfaces**. *Nano Lett* 2020, **20**:6364–6371.
Developed a general methodology to create IR nanospectroscopy platforms for characterization of metal-oxide/electrolyte interfaces.

84. ** Nepel TCM, Anchieta CG, Cremasco LF, Sousa BP, Miranda AN, Oliveira LCCB, Francisco BAB, Júlio JpdO, Maia FCB, Freitas RO, *et al.*: **In situ infrared micro and nanospectroscopy for discharge chemical composition investigation of non-aqueous lithium–air cells**. *Adv Energy Mater* 2021, **11**, 2101884.
First IR nanospectroscopy of an electrochemical three-phase zone.

85. ** He X, Larson JM, Bechtel HA, Kostecki R: **In situ infrared nanospectroscopy of the local processes at the Li/polymer electrolyte interface**. *Nat Commun* 2022, **13**:1398.
First *in situ* IR nanospectroscopy of energy storage solid/solid interfaces and SEIs.

86. ** Lu YH, Larson JM, Baskin A, Zhao X, Ashby PD, Prendergast D, Bechtel HA, Kostecki R, Salmeron M: **Infrared nanospectroscopy at the graphene-electrolyte interface**. *Nano Lett* 2019, **19**:5388–5393.
First *in situ* and *operando* IR nanospectroscopy of solid-liquid electrolyte interfaces. Discovered a general methodology to create IR nanospectrsocy platforms for characterization of electrochemically controlled interfaces.